






Characteristics of TiO_2 , Cu_2O , and $\text{TiO}_2/\text{Cu}_2\text{O}$ thin films for application in PV devices

Cite as: AIP Advances 9, 055206 (2019); <https://doi.org/10.1063/1.5093037>

Submitted: 16 February 2019 . Accepted: 19 April 2019 . Published Online: 08 May 2019

P. Sawicka-Chudy, M. Sibiński, R. Pawełek , G. Wisz , B. Cieniek , P. Potera, P. Szczepan, S. Adamiak , M. Cholewa, and Ł. Głowa 



View Online



Export Citation



CrossMark

AVS Quantum Science

Co-published with AIP Publishing



Coming Soon!

Characteristics of TiO_2 , Cu_2O , and $\text{TiO}_2/\text{Cu}_2\text{O}$ thin films for application in PV devices

Cite as: AIP Advances 9, 055206 (2019); doi: 10.1063/1.5093037

Submitted: 16 February 2019 • Accepted: 19 April 2019 •

Published Online: 8 May 2019



P. Sawicka-Chudy,^{1,a)} M. Sibiński,² R. Pawełek,³ G. Wisz,⁴ B. Cieniek,⁴ P. Potera,⁴ P. Szczepan,⁴ S. Adamiak,⁴ M. Cholewa,¹ and Ł. Głowa¹

AFFILIATIONS

¹Department of Biophysics, Faculty of Mathematics and Natural Sciences, University of Rzeszow, Pigonia 1 Street, Rzeszow 35-317, Poland

²Department of Semiconductor and Optoelectronic Devices, Lodz University of Technology, Wólczajska 211/215 Street, Lodz 90-924, Poland

³Lodz University of Technology, Institute of Electrical Power Engineering, Stefanowskiego 18/22 Street, Lodz 90-924, Poland

⁴Department of Experimental Physics, Faculty of Mathematics and Natural Sciences, University of Rzeszow, Pigonia 1 Street, Rzeszow 35-317, Poland

^{a)}E-mail: psawicka@ur.edu.pl

ABSTRACT

Several Cu_2O and TiO_2 thin films and four additional $\text{TiO}_2/\text{Cu}_2\text{O}$ structures were fabricated by direct current (DC) magnetron sputtering. The process parameters were selected on the basis of earlier studies and numerical simulations. We examined the morphology of a cross-section of the PV structures, roughness and topography, and the transmission spectra of the thin films. Additionally, the properties of the samples were determined by X-ray diffraction. Next, the morphology cross-sectional and layer compositions of the solar cells was evaluated by scanning electron microscopy. Only one of the $\text{TiO}_2/\text{Cu}_2\text{O}$ structures appeared smooth and homogeneous with columnar-type growth. For the as-grown films, diffraction peaks were observed and identified as brookite, rutile, CuO , and Cu_2O and the average roughness of the samples was 0.5, 1.2, 5.4, and 4.0 nm, respectively. Finally, the transmission spectra of the thin films were recorded. Transmission and reflection spectra of ultraviolet-visible spectroscopy were analyzed, and the optical band gap and absorption coefficient of the oxidized layers were calculated. In the region of 400 to 1000 nm, transmittance varied from 5% to 70% in the TiO_2 samples, and from 15% to 40% in the Cu_2O samples, and reflectance of the TiO_2 and Cu_2O samples ranged from 20% to 90%. In the region of 1.5 eV to 3.5 eV, the mean absorption coefficient varied from $\sim 10^5$ 1/cm to $\sim 3 \cdot 10^5$ 1/cm for TiO_2 thin film, and from $\sim 2 \cdot 10^5$ to $\sim 6 \cdot 10^5$ 1/cm for Cu_2O thin film. The optical band gap values of the samples shifted slightly toward bulk anatase-3.5 eV, bulk rutile-3.1 eV, and copper(I) oxide. Finally, silver contacts were used for the electrodes. One of the fabricated $\text{TiO}_2/\text{Cu}_2\text{O}$ PV structures was found to be sensitive to electromagnetic radiance during the experiment.

© 2019 Author(s). All article content, except where otherwise noted, is licensed under a Creative Commons Attribution (CC BY) license (<http://creativecommons.org/licenses/by/4.0/>). <https://doi.org/10.1063/1.5093037>

I. INTRODUCTION

Researchers from around the world are searching for cheaper materials, low-cost processing, and thinner or more efficient photovoltaic (PV) devices. Metal oxide (MO) semiconductors are one group of new low-cost materials with great potential for PV application.¹ MO semiconductors have high photosensitivity and a non-toxic nature for remediation of environmental pollution and solar

energy conversion. The development of MO solar cells, however, has been very limited. Over the last few years, great attention has been focused on titanium dioxide (TiO_2) thin films. These structures present nontoxic nature; photocatalytic properties after ultraviolet light irradiation; high refractive index, good mechanical, good chemical stability.² Copper oxide (Cu_2O) presents non-toxic nature, abundant availability³ and simple preparation process among oxides.¹

In the present study, we analyzed only the basic properties of TiO_2 and Cu_2O thin films, and a $\text{TiO}_2/\text{Cu}_2\text{O}$ thin-film heterojunction for the future fabrication of solar cells. TiO_2 , as one of the most important n-type semiconductors, has a wide band gap of up to 3.54 eV (brookite) and semiconductor affinity of 1.6 eV. TiO_2 particles serve as the active material for capturing photons and then generating electron-hole pairs. Titanium dioxide is especially used in dye-sensitized solar cells, where dye is the active material that produces electrons and titanium (IV) becomes an injection media for electrons produced by the dye. The energy conversion efficiency of dye-sensitized solar cells is only $\sim 11\%$.⁴ The lifetime use of synthetic dye and expensive platinum as a counter electrode are limitations to dye-sensitized solar cells.⁵ Cu_2O and CuO are p-type semiconductors with a narrower band gap in the range from 1.0 to 2.6 eV. CuO and Cu_2O particles work to widen the spectrum of light of TiO_2 so it can capture more photons. CuO and Cu_2O provide many tracks for the electrons that form on the conduction band of the TiO_2 surface. Electrons will easily and quickly move toward the electrode due to the Schottky barrier⁶ occurring on the TiO_2/CuO -copper interface. $\text{Cu}_2\text{O}/\text{TiO}_2$ and CuO/TiO_2 p-n junctions have emerged as promising materials for optoelectronics, and these materials are potentially useful for cheap and competitive solar cell construction. TiO_2 and Cu_2O thin films can also be prepared using similar techniques.^{5,7} In Table I the information shows the authors, year and techniques of performance of TiO_2 and Cu_2O films.^{8–28}

DC magnetron sputtering as is one of the best techniques for depositing thin films due to the controlled chemical composition, and achieved a high deposition rate and high-quality thin films at low substrate temperatures.²⁹ Furthermore, it is an industrial process that is applicable to large-area deposition.²

There are many reports of metal-semiconductors used for heterojunction solar cells (e.g., $\text{TiO}_2/\text{Cu}_2\text{O}$). Conversion efficiency is the most important property in PV devices.¹ Although the theoretical limit of the energy conversion efficiency of a TiO_2/CuO solar cell is 20%,^{1,7,30} the highest efficiency obtained is much smaller. Several other groups have reported the construction of $\text{CuO}(\text{Cu}_2\text{O})/\text{TiO}_2$ solar cells prepared using various technologies with efficiencies ranging from 0.0005% to 1.62%.^{5,31–35}

Here we evaluated the process parameters of Cu_2O and TiO_2 structures by DC magnetron sputtering. Various parameters were tested and compared to observe their influence on the optical parameters, morphology, composition, and structure in thin films and $\text{TiO}_2/\text{Cu}_2\text{O}$ solar cells. Technologic modifications were aimed at improving copper oxides and titanium oxide for use as active and buffer layers in PV devices for potential application in semiconductor solar cells such as $\text{Cu}_2\text{O}/\text{TiO}_2$ and CuO/TiO_2 .

Specific problems and questions include:

1. What are the structural, optical, and surface properties of the $\text{TiO}_2/\text{Cu}_2\text{O}$ heterojunction and TiO_2 , Cu_2O thin films in the various and selected process parameters?

TABLE I. Authors, year, and preparation method of titanium dioxide and copper oxide films.^{8–28}

Titanium dioxide		
Author (year)	Preparation method	Ref.
N. Ozer et al. (1991)	Metallo-organic sol-gel	8
J. A. Byrne et al. (1998)	Electrophoretic deposition	9
J. H. Kim (1999)	Pulsed laser deposition	10
H. Kikuchi et al. (2006)	Reactive radio frequency sputtering	11
J. Zheng et al. (2014)	Reactive DC sputtering	12
P. Sawicka-Chudy et al. (2018, 2019)		13
W. Z. Shenglong et al. (2008)	Chemical vapor deposition	14
L. J. Meng et al. (1993)		15
G. A. Battiston (1994)		16
N. Rausch et al. (1993)	Sol-gel	17
Z. Starowicz et al. (2018, 2015)		18, 19
Copper oxide		
Author (year)	Preparation method of Cu ₂ O	Ref.
J. Morales et al. (2005)	Spray pyrolysis technique	20
A. Nalbant et al. (2013)	Spin coating	21
H. Zhang et al. (2013)	Dip coating	22
P. Markworth et al. (2001)	Chemical vapor deposition	23
A.Chen et al. (2009)	Pulsed laser deposition	24
S.C.Ray et al. (2001)	Sol-gel	25
P. Sawicka-Chudy et al (2018, 2019)	Reactive DC sputtering	26–28

- How do the process parameters influence the structural, optical, and surface properties of Cu_2O , TiO_2 , and $\text{TiO}_2/\text{Cu}_2\text{O}$?
- How can the performance of $\text{TiO}_2/\text{Cu}_2\text{O}$ solar cells and TiO_2 , Cu_2O thin films be optimized?

II. EXPERIMENTAL

Several Cu_2O and TiO_2 structures were deposited by DC magnetron sputtering using metal Cu and Ti targets. For the substrate materials, we used commercial n-type Si (100) wafers and glass slides with indium tin oxide (ITO). We present two representative layers of TiO_2 (called A1, A2) and Cu_2O (called B1, B2) from a series of studies. The $\text{TiO}_2/\text{Cu}_2\text{O}$ thin-film heterojunctions were fabricated using a two-step process. TiO_2 layers were deposited by DC magnetron sputtering on a commercially available glass substrate at 423.15 K from a Ti target (purity N 99.995%, diameter of 253 mm) in a mixed Ar (99.9999%) and O_2 (99.999%) atmosphere. The base pressure of the deposition chamber was kept at $5.0 \cdot 10^{-4}$ Pa. The process pressure was maintained at ~ 2.6 and ~ 7.4 Pa and the distance between the source and substrate was set as 53 and 58 mm for A1 and A2, respectively. The depositions were conducted for a deposition time of 30 min, at a DC power of 120 W, and with a fixed gas of $4 \text{ cm}^3/\text{s}$ Ar flow rate and $1.5 \text{ cm}^3/\text{s}$ O_2 flow rate for A1 and $0.9 \text{ cm}^3/\text{s}$ Ar flow rate and $1.0 \text{ cm}^3/\text{s}$ O_2 flow rate for A2. Then, p-type Cu_2O was deposited onto the TiO_2 thin layers by DC magnetron sputtering. Although the samples were hardly comparable, the process parameters were selected on the basis of earlier studies and numerical simulations.³⁶ We manufactured four photovoltaic structures: A1B1, A1B2, A2B1, and A2B2. A schematic of the n- TiO_2 /p- Cu_2O structure is shown in Figure 1 and the process parameters are shown in Table II.

The basic material properties, such as the thickness of the thin film, were examined first using the ContourGT surface profiler and morphology with a cross-section of the thin films was analyzed with a scanning electron microscope (SEM) (Tescan Vega3) with energy-dispersive X-ray spectroscopy (EDS) to study the surface composition. Then, the properties of the samples were determined by X-ray diffraction (XRD) on a Bruker XRD D8 Advance diffractometer with Cu-K α (K α average = 1.54178 \AA) radiation. Additionally, roughness and topography were evaluated by atomic force microscopy (AFM). Finally, the transmission spectra of the thin films were recorded using a CARY 5000 spectrophotometer for wavelengths ranging from 200 to 1000 nm.

The average thickness of layers A1, A2, B1, and B2 was 200 nm, 250 nm, 1050 nm, and 3500 nm, respectively. The thickness of the

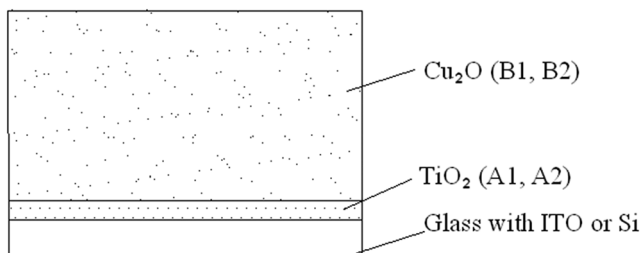


FIG. 1. Scheme of the $\text{TiO}_2/\text{Cu}_2\text{O}$ structure.

TABLE II. Process parameters.

Parameter	A1	A2	B1	B2
Material	TiO_2	TiO_2	Cu_2O	Cu_2O
Thickness of layer [nm]	~ 200	~ 250	~ 1050	~ 3500
Time [min]	30	30	40	60
Power [W]	120	120	80	70
Pressure process [Pa]	2.58	7.36	1.73	2.50
The distance between the source and substrate [mm]	53	58	38	58
Oxygen flow rates [cm^3/s]	1.5	1.0	3.0	8.0
Argon flow rates [cm^3/s]	4.0	0.9	2.0	2.0
Substrate temperature [K]	423	473	473	473

thin films decreased with an increased distance between the source and substrate. Rabih noticed similar behavior in TiO_2 films produced by DC magnetron sputtering.³⁷ The density of the plasma flux increases with a decrease in the distance, which leads to increased collisions between plasma components. Thus, the average energy of impinging atoms is reduced.³⁷ Average values of grain size increase with a decrease in the distance between the source and substrate, as confirmed in an XRD study. Sample A1 was the most uniform due to the lower substrate temperature.

III. RESULTS AND DISCUSSION

A. Morphological properties and EDX

Figure 2 shows SEM images at 15 kV of the A1, A2, B1, and B2 samples with EDS spectrum and an atomic percent [%]. Figure 3 shows cross sections of $\text{TiO}_2/\text{Cu}_2\text{O}$ (A1B1, A2B1, A1B2, A2B2).

A1 and B1 were quite similar to A2 and B2, respectively (Fig. 2). B1 and B2 were much more porous and granular than A1 and A2. Both the B1 and B2 samples comprised individually packed grains. The EDS results confirmed the presence of Ti, O, and Cu in A1 and A2, and O in B1 and B2. The mass percent of O relative to Ti in sample A1 compared with sample A2 was 7 (5.2/0.7) times higher and the presence of elements other than Ti and O accounted for the small thickness of the A1 structure.

Analysis using SEM cross-sections showed that only the cross-section of A1B1 appeared smooth and homogeneous with a columnar-type growth. The columnar surface improved PV devices due to increasing the contact area between the active layer and buffer layer, which allows for more efficient hole injection.³⁸ In the A2B2 sample, the border between TiO_2 and CuO was clearly visible due to its large atomic stresses and strains. Increasing the thickness of the Cu_2O layer led to greater uniformity and less deformation.

B. AFM surface morphologies of TiO_2 and Cu_2O

AFM imaging was used to study the surface topography of TiO_2 and Cu_2O thin films. The measurements were performed in contact mode, at room temperature, in air, using the AFM from CSM

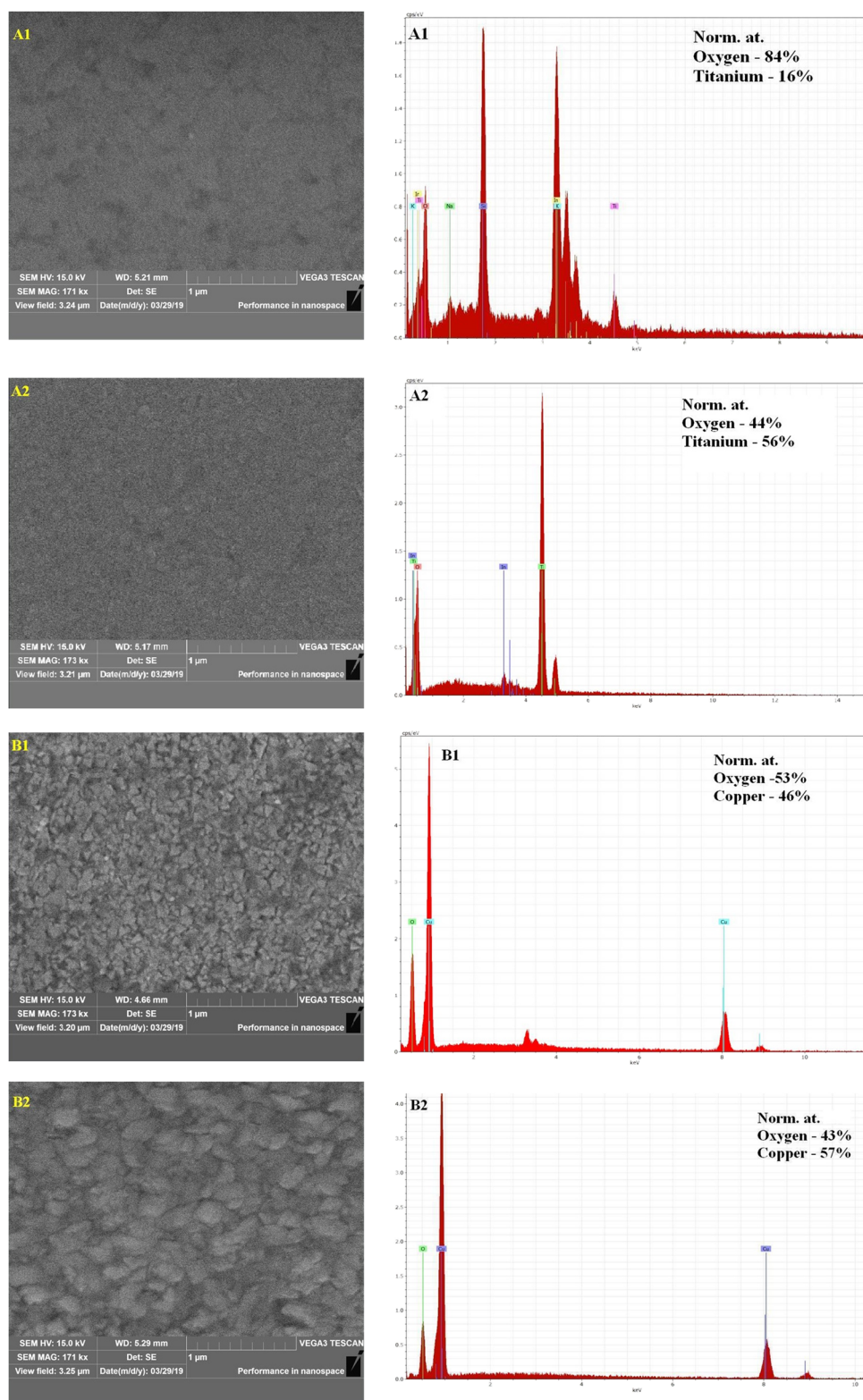


FIG. 2. SEM images of A1, A2, B1, and B2 samples and the corresponding EDS spectrum.

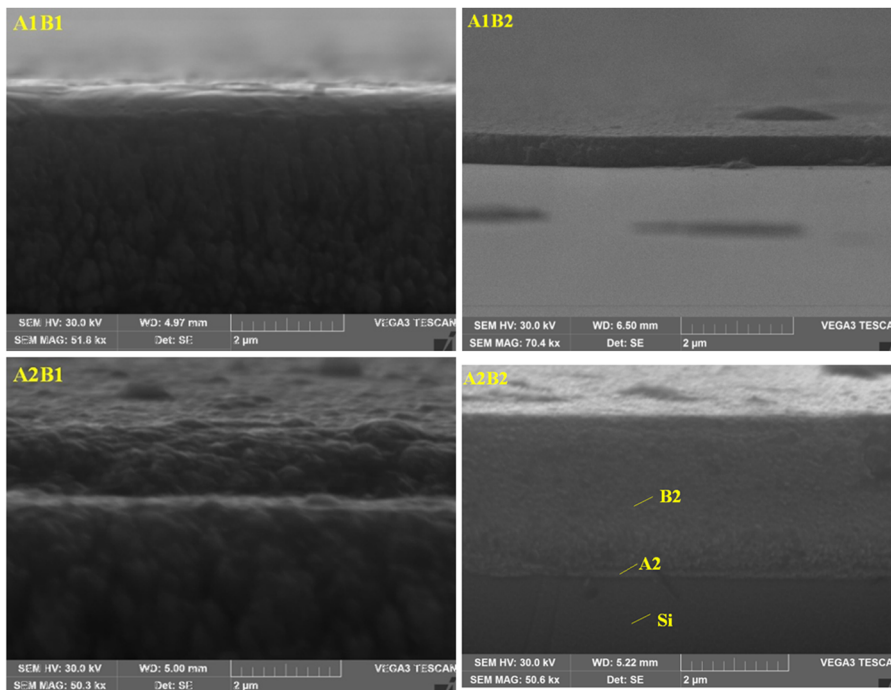


FIG. 3. Cross-sections of A1B1, A1B2, A2B1, A2B2.

Instruments with rotated monolithic silicon AFM Tip - Contr-50. Figure 4 shows the AFM two-dimensional images and their surface profiles taken from A1, A2, and B1, B2 thin films, respectively. The studied surfaces have an area of $4 \times 4 \mu\text{m}^2$. Values of average roughness (Ra) are shown in Table III.

The surface roughness profiles of thin films shown in Figure 4 revealed that the shape and spatial periods of the roughness were very different. A1 appeared less rough than A2 and B1 was less rough than B2. The average roughness was 0.5, 1.2, 5.4, and 4.0 nm, respectively. We conclude that the surface roughness of the coating increases with the thickness of the layer. This finding is in good agreement with the data obtained by Leprince-Wang et al.³⁹ All structures for PV applications should have a low roughness value to minimize degradation of the structure and reduce the probability of dispersing minority carriers.⁴⁰ Based on our analysis of the AFM surface morphologies, we concluded that samples A1 and B2 had better optical quality than samples A2 and B1.

C. XRD analysis

All thin films were analyzed using XRD measurements. To analyze the XRD data, we used the free mathematical software MATCH! Phase Identification from Powder Diffraction (v.3.6) with Crystallography Open Database and Bruker Diffrac. EVA (v4.3) and the ICDD PDF-2 2012 database for comparison. Table IV shows crystalline and amorphous samples.

For the as-grown films, four diffraction peaks were observed and identified as brookite and rutile with (032) and (002), and (211) and (220) crystal directions, respectively for A1 and A2. For B2, five diffraction peaks were observed and identified as Cu_8O with

(020), (202), (022), and (024) crystal directions, and as Cu_2O with a (220) crystal direction (see Fig. 5). Some researchers also observed Cu_8O .^{41–44} In Cu_8O , the oxygen atoms are located at interstitial sites in the Cu lattice.⁴¹ Richardson et al.⁴² reported that Cu_8O is partially oxidized copper on the surfaces.⁴³

We estimated the crystallite size of the sample using Scherrer's formula.^{40,45} For A1 and A2, the strongest peak in the XRD spectrum represents the (002) crystal direction rutile TiO_2 at $61.8^\circ 2\theta$. The grain size of A1 and A2 evaluated from the dominant (002) diffraction peak and calculated using Scherrer's formula was ~ 211 nm and 215 nm, respectively. For B2, the strongest peak in the XRD spectrum represents the (220) crystal direction Cu_2O at $35.5^\circ 2\theta$. The grain size was ~ 28 nm. We could not determine the grain size of B1. Pavan et al. reported a similar crystallite size in experimental Cu_2O thin films.⁴⁶

D. Optical properties

The influence of process parameters on the optical transmittance (T), reflectance (R), absorption coefficient (α) and band gap (E_g) values of the TiO_2 and Cu_2O thin films were evaluated. The transmittance of the structures was studied for wavelengths ranging from 200 to 1000 nm. The optical transmission spectra of A1, A2, B1, B2 and A1B1, A1B2, A2B2 and A2B2 samples are shown in Figure 6.

The highest transparency (up to $\sim 70\%$) was for A1. The mean optical transparency for A2 was between 1% and 5% in the region of 400 to 600 nm. The main mechanism of light trapping in TiO_2 films involved light scattering because TiO_2 is a small absorbent material.¹² The low transmittance values of A2 are due to the small oxygen and argon flow rate values – $1.0 \text{ cm}^3/\text{s}$ and $0.9 \text{ cm}^3/\text{s}$,

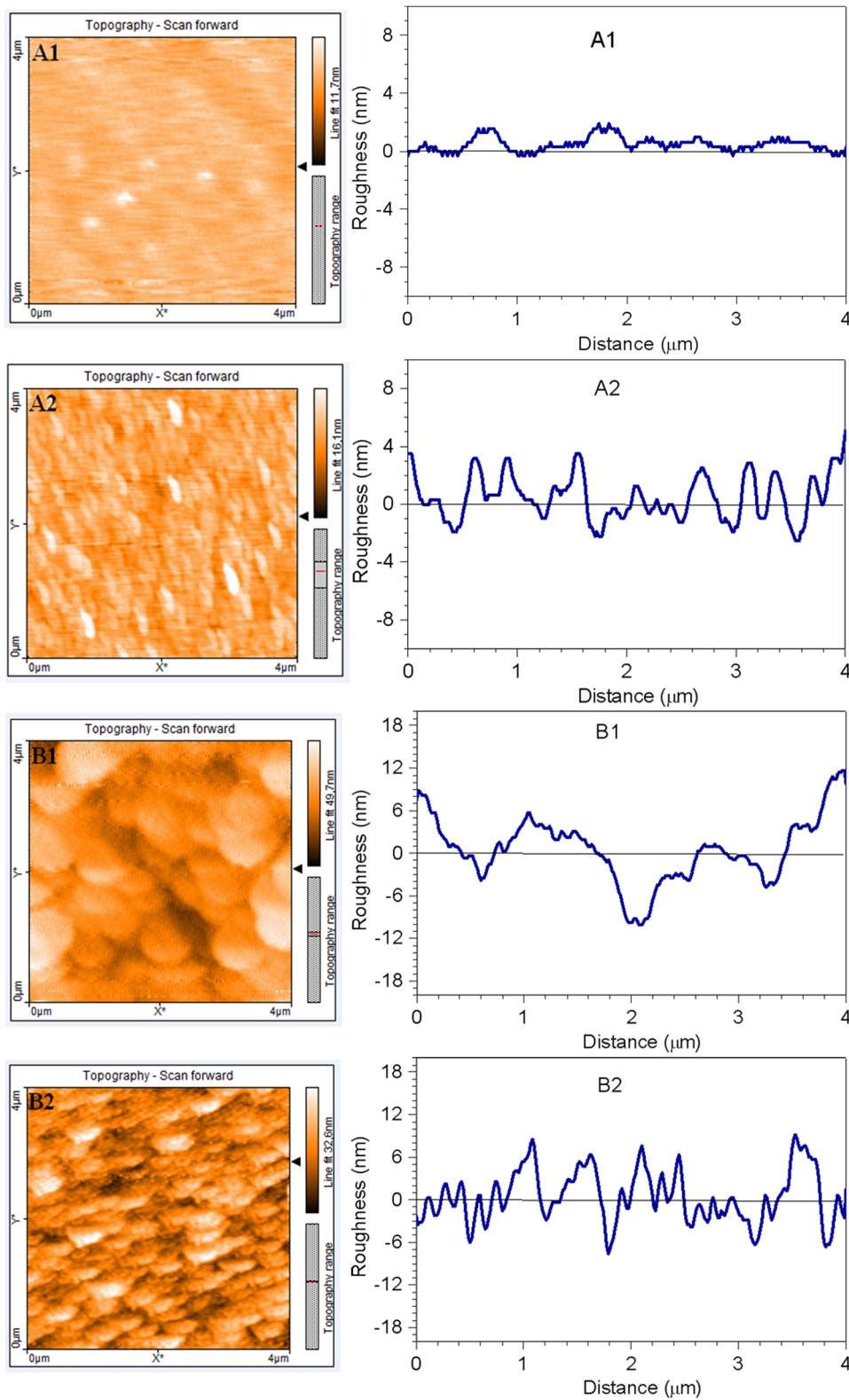


FIG. 4. AFM morphological images (left) and surface roughness profiles (right) of samples A1, A2, B1 and B2.

TABLE III. Average roughness of samples A1, A2, B1, and B2.

Sample	Ra [nm]
A1	0.5
A2	1.2
B1	5.4
B2	4.0

TABLE IV. Crystalline and amorphous of A1, A2, B1, B2 samples.

Sample	Crystalline [%]	Amorphous [%]
A1	58.7	41.3
A2	52.3	47.7
B1	70.3	29.7
B2	55.7	44.3

respectively. Venkataraj et al.⁴⁷ and Zhang et al.⁴⁸ also reported that increasing the gas flow rates leads to an increase in film transparency.

The mean optical transparency of Cu₂O thin films increased from 15% to 40% in the region of 600 to 1000 nm, which was due to an increase in the sputtering pressure from 1.73 to 2.5 Pa. By increasing the sputtering pressure, the defect center density decreased and increased the transmittance value.⁴⁹ The defect centers present in the structures scattered the light and decreased the transmittance values

at low sputtering pressures. Meng et al.⁵⁰ and Reddy et al.⁵¹ studied similar behavior in Cu₂O films and ZnO films, respectively.

Figures 7 shows the reflection spectra (R) of TiO₂, Cu₂O, and TiO₂/Cu₂O. The reflectance of TiO₂ (A2) had the highest value (~90%) in the region of 200 to 250 nm. In the region of 400 to 1000 nm, the mean optical reflectance for sample A1 was ~20%, and for sample A2, ~20%; for samples B1 and B2, the reflectance was 20%. The different reflection spectra of thin films were due to differences in light scattering and crystal size effect.⁵¹

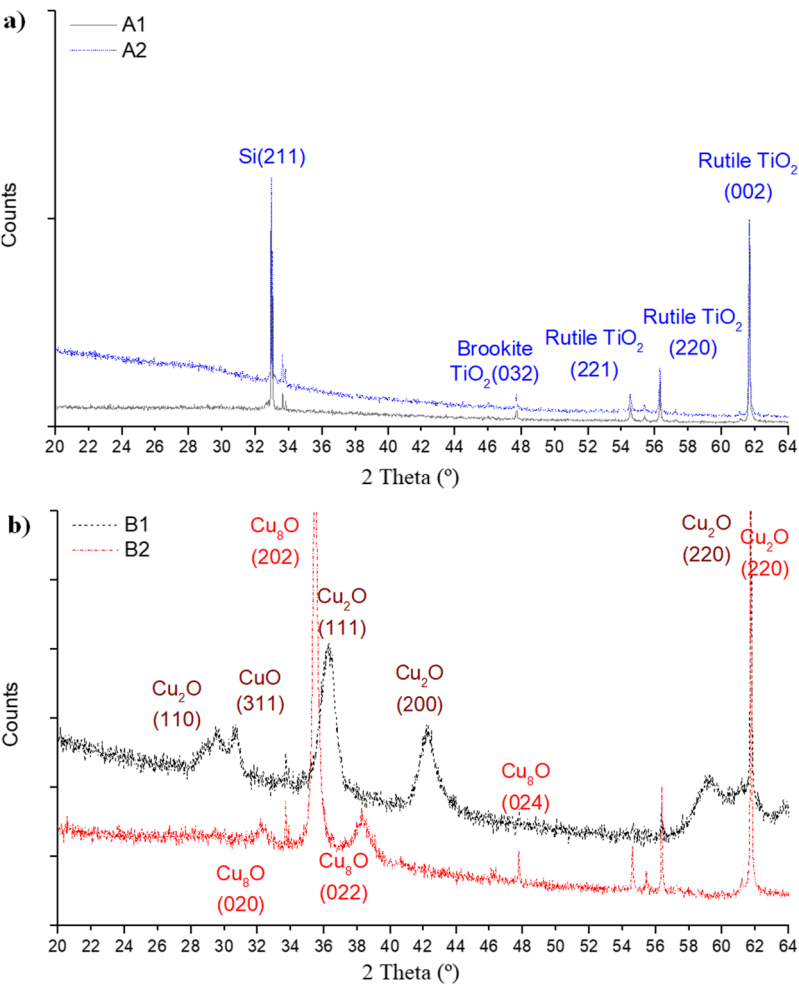


FIG. 5. XRD spectra of a) A1 and A2, and b) B1 and B2 thin films.

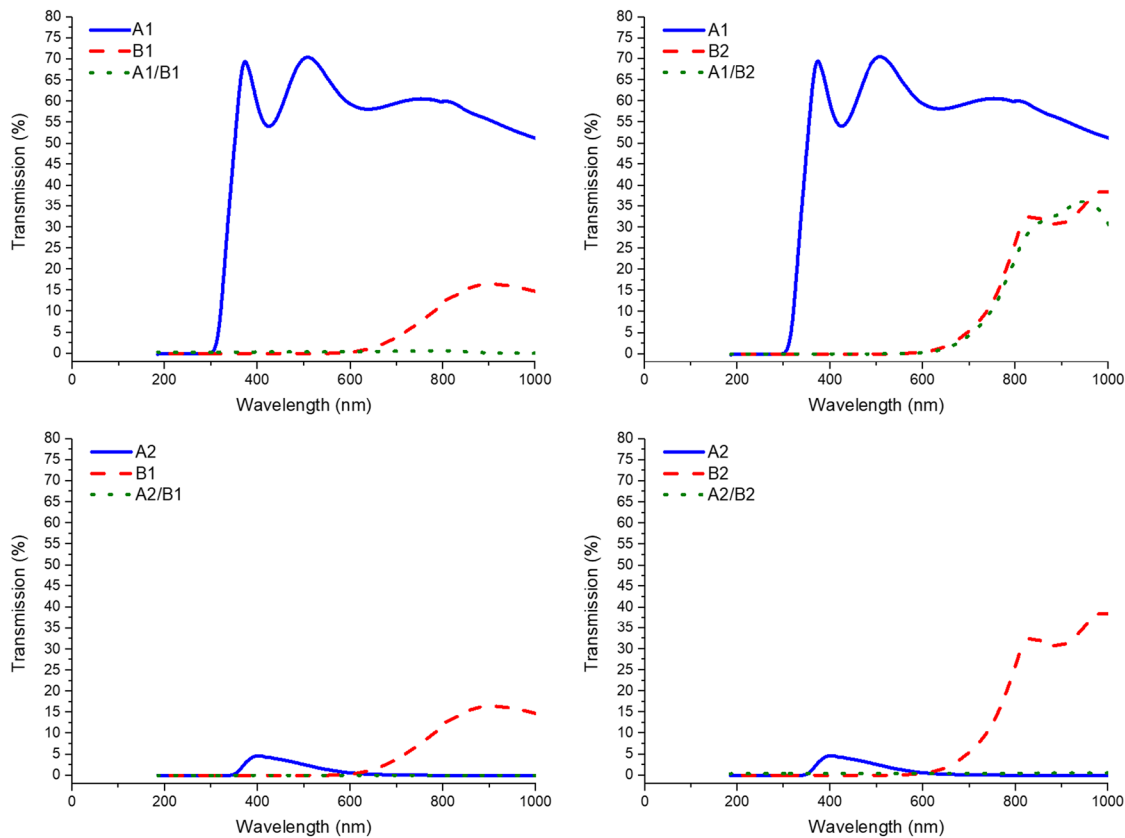


FIG. 6. Optical transmission spectra of the A1, A2, and B1, B2, A1/B1, A1/B2, A2/B1, and A2/B2 samples.

We calculated absorption coefficient (α) by the following relation:⁵²

$$\alpha \approx \frac{1}{d} \ln\left(\frac{1-R}{T}\right) \quad (1)$$

where d is the thickness of the film, and T is its transmittance region. Figure 8 shows the absorption coefficient for the samples.

As shown in Figure 8, the mean absorption coefficient for sample A1 was below $1 \cdot 10^5$ 1/cm. The absorption coefficient affects the transmittance of thin films (formula 1). In the region of 2 eV to 3.5 eV, the transmittance of sample A2 ranged from $\sim 2 \cdot 10^5$ to $\sim 3 \cdot 10^5$ 1/cm; for samples B1, B2, transmittance ranged from $\sim 2 \cdot 10^5$ to $\sim 6 \cdot 10^5$ 1/cm and from $\sim 2.5 \cdot 10^5$ to $\sim 3.5 \cdot 10^5$ 1/cm, respectively. These values are in fairly good agreement with the data obtained by Ito et al.^{53,54} in the energy range from 2.1 to 2.5 eV.

The optical band gap energy (E_g) of films was determined using the following equation:⁵³

$$\alpha h\nu = A(h\nu - E_g)^m, \quad (2)$$

where α is absorbance, $h\nu$ is photon energy, and A is the band tailing parameter. For Cu_2O , the value of m should be taken as 2, according to theoretical and experimental results.⁵¹ For TiO_2 , the value of m should be taken as $1/2$, based on theoretical and experimental results.⁵² To calculate the indirect and direct band gap, $(\alpha h\nu)^2$ and

$(\alpha h\nu)^{1/2}$ are plotted as a function of photon energy $E = h\nu$, shown in Figure 10.

Figure 9 shows that the E_g values of the samples shifted slightly toward bulk brookite – 3.5 eV (A1)^{12,55} and bulk rutile – 3.1 eV (A2).⁵⁵ The optical band gap values of the B1 and B2 samples shifted slightly toward copper(II) oxide – 1.9 eV and copper(I) oxide – 2.3 eV. The optical band gap is in fairly good agreement with the literature data reported by Reddy et al.⁵⁶ The results are in agreement with the XRD analysis.

E. I-V characteristics of $\text{TiO}_2/\text{Cu}_2\text{O}$ thin-film heterojunction

Finally, two silver contacts for the $\text{TiO}_2/\text{Cu}_2\text{O}$ structures were attached to the Cu_2O and ITO using conductive glue. Measurements of the I-V characteristics were obtained in the dark and under illumination ($\sim 1000 \text{ W/m}^2$) using a Keithley 2062. Only A2B1 was found to be sensitive to electromagnetic radiance during the experiment (Fig. 10). Unfortunately, photovoltaic I-V function was not observed. To the best of our knowledge, other groups have fabricated $\text{TiO}_2/\text{Cu}_2\text{O}$ solar cells and observed efficiencies up to only 1.61%.⁵

We suspect that the lack of efficiency may be due to an excessively thick (B1 \sim 1050, B2 \sim 3500 nm) absorber layer and poor

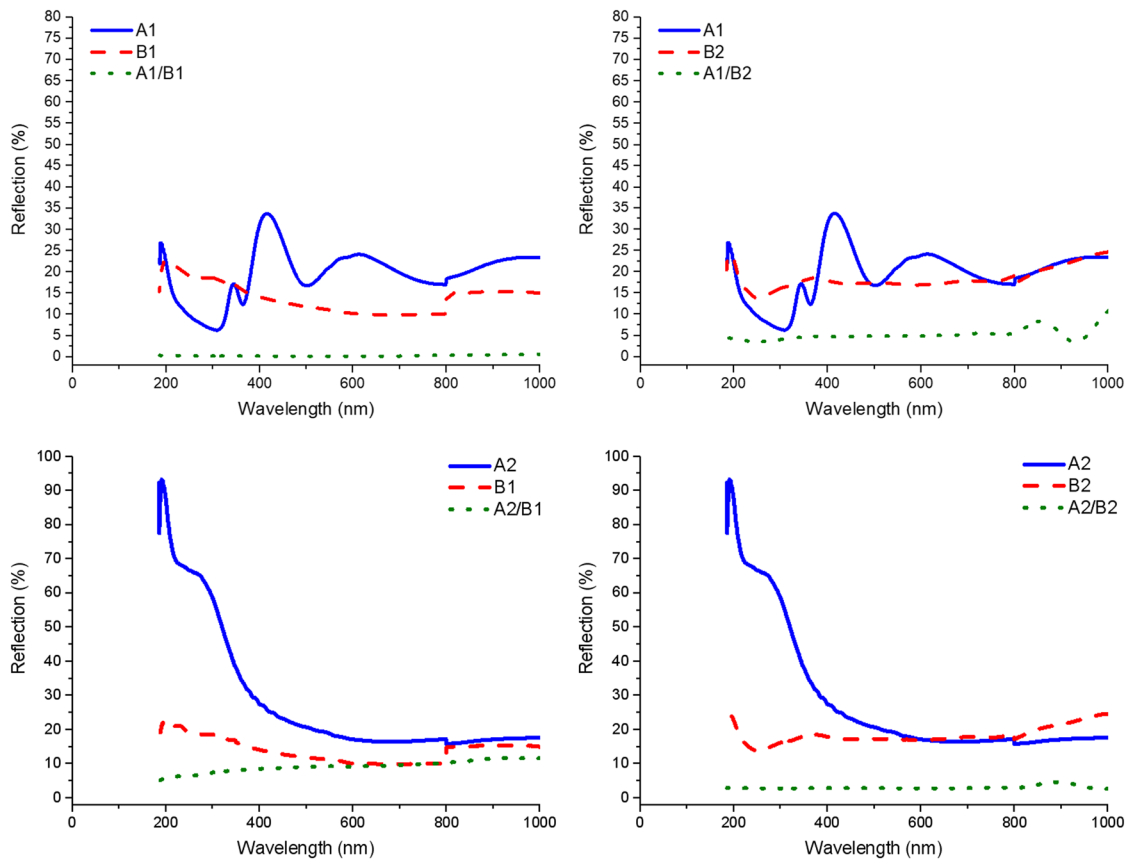


FIG. 7. Reflection spectra of the samples (A1, A2, B1, B2, A1B1, A1B2, A2B1, A2B2) on the thin film.

contact and thin film quality. In addition, steps should be taken to avoid the formation of CuO and Cu_2O , improve the crystallinity of Cu_2O ,⁵⁷ synthesize larger Cu_2O grains,⁵⁸ and improve the electrodes. Several authors have proposed various aspects to

improve the performance of $\text{TiO}_2/\text{Cu}_2\text{O}$ structures. Rokhmat et al. used a NaOH post-treatment to further improve the efficiency of solar cells.⁵⁸ Li et al. proposed using anti-reflection coatings, textured electrodes, and quantum dots.³⁴ Ichimura et al. improved the

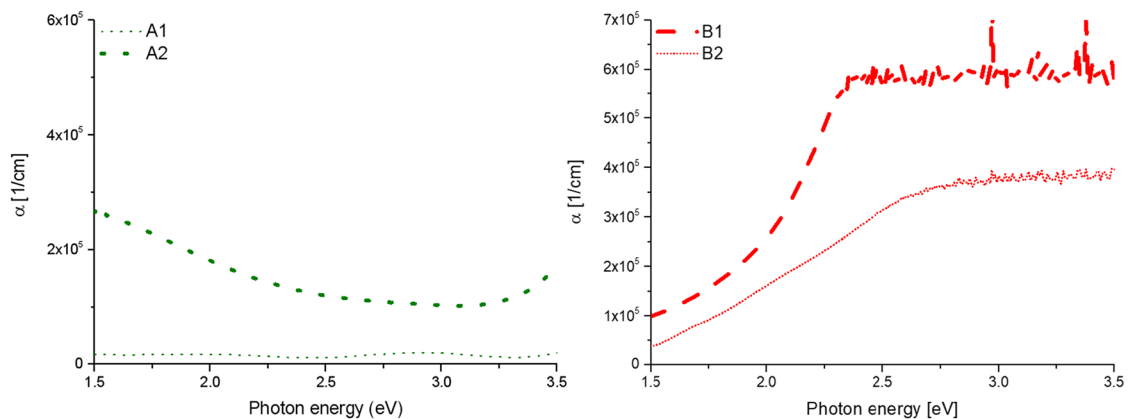


FIG. 8. The absorption coefficient for the samples (A1, A2, B1, B2).

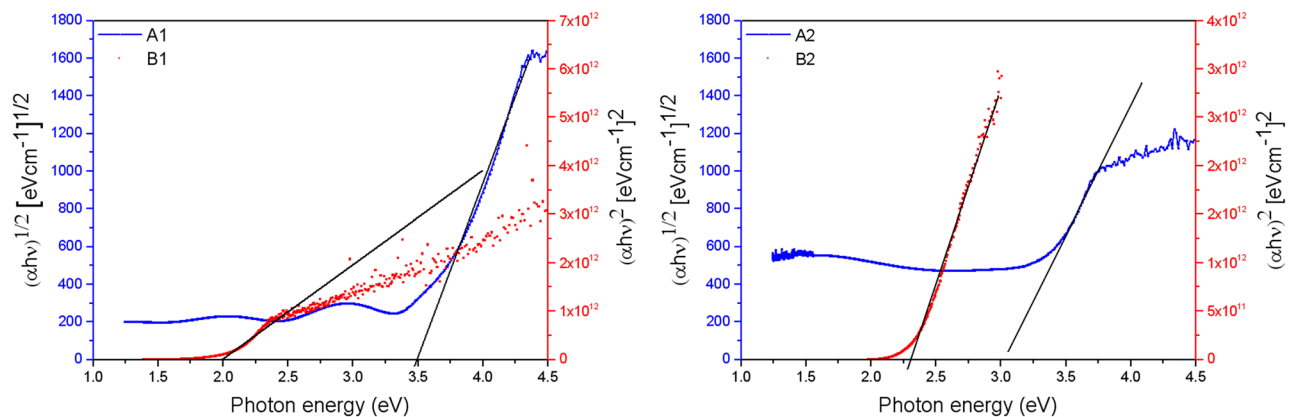


FIG. 9. Optical absorption coefficients α of the samples (A1, A2, B1, B2) as a function of incident photon energy by indirectly and directly allowed transitions.

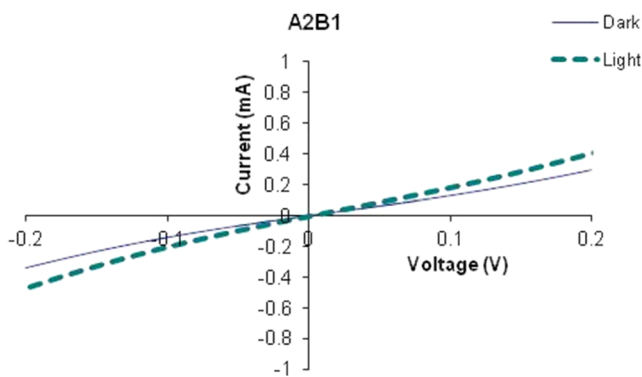


FIG. 10. I-V characteristics of $\text{TiO}_2/\text{Cu}_2\text{O}$ heterojunction solar cells.

performance of solar cells by annealing at 120°C .⁵⁷ Masudy-Panah et al. reported that the photocurrent in CuO absorber layer thin films degraded at a thickness of 700 nm and proposed an optimum thickness of ~ 550 nm.⁵⁹ Studies to improve the prototype of solar cell $\text{TiO}_2/\text{Cu}_2\text{O}$ by taking into account the above-mentioned aspects are planned.

IV. CONCLUSIONS

A summary of the results of all the thin films A1, A2, B1, and B2 is presented in Table V. This preliminary analysis indicates that among the manufactured TiO_2 thin films, A1 was the most promising as a buffer layer. It was uniform and contained few defects. Values of surface roughness, reflectance, and the absorption coefficient were smaller for A1 than for A2. Additionally, A1 was more

TABLE V. Summary results of all thin films A, A2, B1, and B2.

Parameter	Sample			
	A1	A2	B1	B2
Thickness of layer [nm]	200	250	1050	3500
Surface properties	Uniform, few defects	Smooth, many different-sized defects	Porous, few defects	Granular, point defects
Type of growth	Not columnar	Columnar	Columnar	Not columnar
Surface roughness [nm]	0.5	1.2	5.4	4.0
Composition (stoichiometry)	TiO_2	TiO_2	Cu_2O	Cu_2O
XRD analysis	Rutile, brookite TiO_2	Rutile, brookite TiO_2	CuO , Cu_2O	Cu_8O
Crystalline [%]	58.9	52.3	70.3	55.7
Grain size [nm]	211	215	-	28
Max. transmittance [%]	70	5	15	40
Max. reflectance [%]	35	98	20	25
Max. absorption coefficient [1/cm]	$0.1 \cdot 10^5$	$3 \cdot 10^5$	$6 \cdot 10^5$	$3.5 \cdot 10^5$
Band gap [eV]	3.5	3.1	1.8	2.3

transparent than A2. On the other hand, based on the manufactured Cu₂O thin films, B1 was the most future-oriented solution for PV application as an absorber layer. It had only a few defects with a columnar type of growth. For films, diffraction peaks were observed and identified as Cu₂O and CuO, and B1 was also more crystalline than B2. Furthermore, the transmittance and reflectance values were smaller but the maximum absorption coefficient was higher than that for B2. B1 was more porous and had a high value of surface roughness. Only the A2B1 thin film, however, was photosensitive.

The main conclusions were as follows:

- the thickness of thin films decreased with an increased distance between the source and substrate,
- substrate temperature influences the uniformity of thin films – with decreasing temperature, thin films become more uniform,
- porous structures are due to small distances between the source and substrate,
- the surface roughness of the coating increases with the thickness of the layer,
- increasing the sputtering pressure increases the transmittance value,
- the low transmittance is due to the small oxygen and argon flow rate values,
- the PV structure exhibited no photovoltaic I-V function, probably due to the insufficient quality of the absorber layer and electrodes.

V. SUMMARY

In conclusion, Cu₂O and TiO₂ thin films and four TiO₂/Cu₂O structures were described. The material properties, such as thickness of the thin film, morphology of the cross-section, XRD analysis, roughness, and topography transmission spectra were examined. We studied the effect of the distance between the source and substrate, substrate temperature, and sputtering pressure on the material properties of the thin films.

Finally, we prepared a PV structure by attaching two silver contacts to the Cu₂O and ITO using conductive glue. Under illumination (~1000W/m²), only one of the PV structures was photosensitive. Improvements to the crystallinity of the Cu₂O thin films and the quality of the contacts for TiO₂/Cu₂O solar cells are planned.

REFERENCES

- ¹L. Zhu, "Development of metal oxide solar cells through numerical modelling," Ph.D. thesis.
- ²Z. Can, D. Wanyu, W. Hualin, C. Weiping, and J. Dongying, "Influences of working pressure on properties for TiO₂ films deposited by DC pulse magnetron sputtering," *Journal of Environmental Sciences* **21**, 741–744 (2009).
- ³H. Zhu, J. Zhang, Ch. Li, F. Pan, T. Wang, and B. Huang, "Cu₂O thin films deposited by reactive direct current magnetron sputtering," *Thin Solid Films* **517**(19), 5700–5704 (2009).
- ⁴B. O'Regan and M. Grätzel, "A low-cost, high-efficiency solar cell based on dye-sensitized colloidal TiO₂ films," *Nature* **353**, 737–740 (1991).
- ⁵M. Rokhmat, E. Wibowo, Sutisna, Khairurrijal, and M. Abdullah, "Performance improvement of TiO₂/CuO solar cell by growing copper particle using fix current electroplating method," *Procedia Engineering* **170**, 72–77 (2017).
- ⁶T. Bora, H. H. Kyaw, S. Sarkar, S. K. Pal, and J. Dutta, "Highly efficient ZnO/Au Schottky barrier dye-sensitized solar cells: Role of gold nanoparticles on the charge-transfer process," *Beilstein J. Nanotechnol.* **2**, 681–690 (2011).
- ⁷P. Sawicka-Chudy, G. Wysz, Sz. Górny, Ł. Głowa, M. Sibiński, and M. Cholewa, "Numerical simulation and analysis of experimental TiO₂/Cu₂O thin film for photovoltaic structures," *Journal of Nanoelectronics and Optoelectronics* **13**, 715–721 (2018).
- ⁸N. Ozer, H. Demiryont, and J. H. Simmons, *Applied Optics* **30**, 3661–3666 (1991).
- ⁹J. A. Byrne, B. R. Eggins, S. Linquette-Mailley, and P. S. M. Dunlop, *Analyst* **123**, 2007–2012 (1998).
- ¹⁰J. H. Kim, S. Lee, and H. S. Im, *Applied Surface Science* **151**–16 (1999).
- ¹¹H. Kikuchi, M. Kitano, M. Takeuchi, M. Matsuoka, M. Anpo, and P. V. Kamat, *Journal of Physical Chemistry B* **110**, 5537–5541 (2006).
- ¹²J. Zheng, S. Bao, Y. Guo, and P. Jin, "TiO₂ films prepared by DC reactive magnetron sputtering at room temperature: Phase control and photocatalytic properties," *Surface & Coatings Technology* **240**, 293–300 (2014).
- ¹³P. Sawicka-Chudy, G. Wysz, Ł. Głowa, M. Sibiński, P. Potera, M. Cholewa, M. Wielgosz, and Sz. Górny, "Optical and structural properties of TiO₂ as intermediate buffer layer prepared by DC reactive magnetron sputtering for solar cells," *Optik* **181**, 1122–1129 (2019).
- ¹⁴W. Z. Shenglong, Z. Ying, and L. F. Wang, "Photocatalytic Zn-doped TiO₂ films prepared by DC reactive magnetron sputtering," *Vacuum* **82**, 328–335 (2008).
- ¹⁵L. J. Meng and M. P. Dossantos, *Thin Solid Films* **226**, 22–29 (1993).
- ¹⁶G. A. Battiston, R. Gerbasio, M. Porchia, and A. Marigo, *Thin Solid Films* **239**, 186–191 (1994).
- ¹⁷N. Rausch and E. P. Borte, *Journal of the Electrochemical Society* **140**, 145–149 (1993).
- ¹⁸Z. Starowicz, K. Gawlińska, J. Walterb, R. P. Sochac, G. Kulesza-Matlaka, and M. Lipińska, "Extended investigation of sol aging effect on TiO₂ electron transporting layer and performances of perovskite solar cells," *Materials Research Bulletin* **99**, 136–143 (2018).
- ¹⁹Z. Starowicz, M. Lipiński, R. P. Socha, K. Berent, G. Kulesza, and P. Ozga, "Photochemical silver nanoparticles deposition on sol-gel TiO₂ for plasmonic properties utilization," *J Sol-Gel Sci Technol* **73**, 563–571 (2015).
- ²⁰J. Morales, L. Sanchez, F. Martin, J. Ramos-Barrado, and M. Sanchez, "Use of low-temperature nanostructured CuO thin films deposited by spray-pyrolysis in lithium cells," *Thin Solid Films* **474**(1–2), 133–140 (2005).
- ²¹A. Nalbant, Ö. Ertek, and İ. Okur, "Producing CuO and ZnO composite thin films using the spin coating method on microscope glasses," *Mater. Sci. Eng. B* **178**, 368–374 (2013).
- ²²H. Zhang, G. Zhao, and L. Xu, "Preparation of the photosensitive copper complex and CuO film pattern," *Appl. Surf. Sci.* **274**, 397–400 (2013).
- ²³P. Markworth, X. Liu, J. Dai, W. Fan, T. Marks, and R. Chang, "Coherent island formation of Cu₂O films grown by chemical vapor deposition on MgO (110)," *J. Mater. Res.* **16**, 2408–2414 (2001).
- ²⁴A. Chen, H. Long, X. Li, Y. Li, G. Yang, and P. Lu, "Controlled growth and characteristics of single-phase Cu₂O and CuO films by pulsed laser deposition," *Vacuum* **83**, 927–930 (2009).
- ²⁵S. C. Ray, "Preparation of copper oxide thin film by the sol-gel-like dip technique and study of their structural and optical properties," *Sol. Energy Mater. Sol. Cells* **68**, 307–312 (2001).
- ²⁶P. Sawicka-Chudy, G. Wysz, Sz. Górny, Ł. Głowa, M. Sibiński, M. Cholewa, and P. Potera, "Numerical simulation and analysis of experimental TiO₂/Cu₂O thin film for photovoltaic structures," *Journal of Nanoelectronics and Optoelectronics* **13**, 715–721 (2018).
- ²⁷P. Sawicka-Chudy, G. Wysz, M. Sibiński, M. Cholewa, P. Potera, Ł. Głowa, and R. Pawelek, "Optical and structural properties of Cu₂O thin film as active layer in solar cells prepared by DC reactive magnetron sputtering," *Arch. Metall. Mater.* **64**(1), 243–250 (2019).
- ²⁸G. Wysz, P. Sawicka-Chudy, P. Potera, M. Sibiński, R. Yavorskyi, Ł. Głowa, B. Cieniek, and M. Cholewa, "Morphology, composition, structure and optical properties of thermal annealed Cu₂O thin films prepared by reactive DC sputtering method," accepted to *Molecular Crystals and Liquid Crystals*.

- ²⁹A. Karapetyan, A. Reymers, S. Giorgio, C. Fauquet, L. Sajti, S. Nitsche, M. Nersisyan, V. Gevorgyan, and W. Marine, "Cuprous oxide thin films prepared by thermal oxidation of copper layer. Morphological and optical properties," *Journal of Luminescence* **159**, 325–332 (2015).
- ³⁰P. Sawicka-Chudy, M. Sibiński, G. Wisz, E. Rybak-Wilusz, and M. Cholewa, Numerical analysis and optimization of $\text{Cu}_2\text{O}/\text{TiO}_2$, CuO/TiO_2 , nanostructures PV using SCAPS, *Journal of Physics: Conference Series* **1033**, conference 1, 1–10 (2018).
- ³¹Y. Luo, L. Wang, Y. Zou, X. Sheng, L. Chang, and D. Yang, "Electrochemically deposited Cu_2O on TiO_2 nanorod arrays for photovoltaic application," *Electrochemical and Solid-State Letters* **15**, H34–H36 (2012).
- ³²A. Mittiga, E. Salza, F. Sarto, M. Tucci, and R. Vasant, "Heterojunction solar cell with 2% efficiency based on a Cu_2O substrate," *Applied physics letters* **88**, 163502 (2006).
- ³³S. Hussain, C. Cao, Z. Usman, Z. Chen, G. Nabi, W. S. Khan, Z. Ali, F. K. Butt, and T. Mahmood, "Fabrication and photovoltaic characteristics of $\text{Cu}_2\text{O}/\text{TiO}_2$ thin film heterojunction solar cell," *Thin Solid Films* **522**, 430–434 (2012).
- ³⁴D. Li, C. Chien, S. Deora, P. Chang, E. Moulin, and J. Lu, "Prototype of a scalable core-shell $\text{Cu}_2\text{O}/\text{TiO}_2$ solar cell," *Chemical Physics Letters* **501**, 446–450 (2011).
- ³⁵A. R. Zainun, T. Sakamoto, U. M. Noor, M. Rusop, and M. Ichimura, "New approach for generating $\text{Cu}_2\text{O}/\text{TiO}_2$ composite films for solar cell applications," *Materials Letters* **66**, 254–256 (2012).
- ³⁶P. Sawicka-Chudy, G. Wisz, L. Glowa, M. Sibinski, P. Potera, M. Cholewa, S. Adamiak, E. Rybak-Wilusz, and B. Cieniek, " TiO_2 grown by pulsed laser deposition and reactive DC direct current sputtering as an intermediate buffer layer in photovoltaic structures," *J. Nanoelectron. Optoelectron.* **13**, 995–1000 (2018).
- ³⁷L. Rabih, K. Triyana, and P. Nurwantoro, "Effect of substrate temperature and target-substrate distance on growth of TiO_2 thin films by using DC-reactive sputtering technique," *Jurnal Fisika Indonesia* No: 49, Vol XVII, Edisi April 2013.
- ³⁸G. Wang, T. Jiu, P. Li, J. Li, C. Sun, F. Lu, and J. Fang, "In situ growth of columnar MoO_3 buffer layer for organic photovoltaic applications," *Organic Electronics* **15**, 29–34 (2014).
- ³⁹Y. Leprince-Wang and K. Yu-Zhang, "Study of the growth morphology of TiO_2 thin films by AFM and TEM," *Surface and Coatings Technology* **140**(2), 155–160 (2001).
- ⁴⁰E. Dumiszewska, P. Knypis, M. Wesołowski, and W. Strupiński, "Wielozłączowe ogniwa słoneczne," *Przegląd Elektrotechniczny* **5**, 215–221 (2014).
- ⁴¹Y. Shen, "Development of thin film photovoltaic cells based on low cost metal oxides," PD thesis, 2014.
- ⁴²R. Guan, H. Hashimoto, and K. H. Kuo, "Electron-microscopic study of the structure of metastable oxides formed in the initial stage of copper oxidation. II. Cu_8O ," *Acta Crystallographica Section B: Structural Science* **40**, 560–566 (1984).
- ⁴³T. J. Richardson, J. L. Slack, and M. D. Rubin, "Electrochromism in copper oxide thin films," *Electrochimica Acta* **46**, 2281–2284 (2001).
- ⁴⁴F. Arith, S. A. M. Anis, M. Said, and M. I. Idris, "Low cost electro-deposition of cuprous oxide P-N homo-junction solar cell," *Advanced Materials Research* **827**, 38–43 (2014).
- ⁴⁵P. Scherrer, *Bestimmung der inneren Struktur und der Größe von Kolloidteilchen mittels Röntgenstrahlen*, in *Kolloidchemie Ein Lehrbuch*, Springer, Berlin, Heidelberg, 1912, pp. 387–409.
- ⁴⁶M. Pavan, S. Rühle, A. Ginsburg, D. A. Keller, H. Barad, P. M. Sberna, D. Nunes, R. Martins, A. Y. Anderson, A. Zaban, and E. Fortunato, " $\text{TiO}_2/\text{Cu}_2\text{O}$ all-oxide heterojunction solar cells produced by spray pyrolysis," *Solar Energy Materials & Solar Cells* **132**, 549–556 (2015).
- ⁴⁷S. Venkataraj, D. Severin, R. Drese, F. Koerfer, and M. Wuttig, *Thin Solid Films* **502**(1–2), 235–239 (2006).
- ⁴⁸W. Zhang, Y. Li, S. Zhu, and F. Wang, "Influence of argon flow rate on TiO_2 photocatalyst film deposited by dc reactive magnetron sputtering," *Surface and Coatings Technology* **182**(2–3), 192–198 (2004).
- ⁴⁹A. Sivasankar Reddy, S. Uthanna, and P. Sreedhara Reddy, "Properties of dc magnetron sputtered Cu_2O films prepared at different sputtering pressures," *Applied Surface Science* **253**(12), 5287–5292 (2007).
- ⁵⁰L. J. Meng and M. P. dos Santos, *Thin Solid Films* **250**, 26 (1994).
- ⁵¹S. Wahyuningsih, G. Fadillah, R. Hidayat, and A. H. Ramelan, "Thin film ZnO coated on FTO/ TiO_2 as an anti reflection coating for enhancing visible light harvesting in dye sensitized solar cells system," *Procedia Chemistry* **19**, 632–637 (2016).
- ⁵²L. J. Meng and M. P. Dossantos, *Thin Solid Films* **226**, 22–29 (1993).
- ⁵³C. Malerba, F. Biccari, C. L. A. Ricardo, M. D'Incau, P. Scardi, and A. Mittiga, "Absorption coefficient of bulk and thin film Cu_2O ," *Solar Energy Materials and Solar Cells* **95**(10), 2848–2854 (2011).
- ⁵⁴T. Ito, T. Kawashima, H. Yamaguchi, T. Masumi, and S. Adachi, "Optical properties of Cu_2O studied by spectroscopic ellipsometry," *J. Phys. Soc. Jpn.* **67**, 2125–213 (1998).
- ⁵⁵X. Hua, Z. Liu, P. G. Bruce, and C. P. Grey, "The Morphology of TiO_2 (B) Nanoparticles," *J. Am. Chem. Soc.* **137**(42), 13612–13623 (2015).
- ⁵⁶A. S. Reddy, G. Venkata, R. S. Uthanna, and P. Sreedhara Reddy, *Materials Letters* **60**(13–14), 1617–1621 (2006).
- ⁵⁷M. Ichimura and Y. Kato, "Fabrication of $\text{TiO}_2/\text{Cu}_2\text{O}$ heterojunction solar cells by electrophoretic deposition and electrodeposition," *Materials Science in Semiconductor Processing* **16**(6), 1538–1541 (2013).
- ⁵⁸M. Rokhmat, E. Wibowo, Sutisna, E. Yuliza, Khairurrijal, and M. Abdullah, "Enhancement of TiO_2 particles based-solar cells efficiency by addition of copper(II) nitrate and post-treatment with sodium hydroxide," *Advanced Materials Research* **1112**, 245–250 (2015).
- ⁵⁹S. Masudy-Panah, R. Siavash Moakhar, C. Sheng Chua, A. Kushwaha, T. I. Wong, and G. Kumar Dalapati, "Rapid thermal annealing assisted stability and efficiency enhancement in a sputter deposited CuO photocathode," *RSC Adv.* **6**, 29383–29390 (2016).